

ICSS(2) : Function and Contribution of Response Modification devices in Reduction of Seismic Action



T. Matsuda

West Nippon Expressway Engineering Kyusyu Limited, Japan

A. Igarashi

Kyoto University, Japan

H. Ouchi, T. Ueda and F. Wada

West Nippon Expressway Company Limited, Japan

M. Sakate

Dohyu Daichi Corporation, Japan

H. Uno

Oiles Corporation, Japan

H. Matsuda

Dohyu Daichi Company Limited, Japan (formerly: JIP Technosciense Corporation, Japan)

SUMMARY

The Isolation Seismic Controlled Slide System (ICSS) is a newly proposed seismic control structure for multi-span continuous girder bridges using slide bearings, elastomeric bearings and energy dissipation devices. Applying this system, the bridge superstructure will be mostly isolated so that the indeterminate force due to temperature change on bearings is gradually reduced, while the seismic response is controlled by elastomeric bearings and seismic dampers installed to a limited number of piers. In this paper, numerical dynamic response analysis is performed to identify the roles for the three devices during earthquake for the example of an 18-span continuous steel girder bridge with 1,200m length. As a result, it is shown that the proposed system ensures sufficient damping capability and stability for all the design earthquake ground motions considered.

Keywords: Seismic isolation control, elastomeric bearing, seismic damper, slide bearing, ICSS

1. INTRODUCTION

The standard design provisions for bridges in Japan described in Specifications for Highway Bridges (Japan Road Association, 2002) prohibits excessive elongation of fundamental period of the bridges in adopting seismic isolation design. This is in consideration of possibility of increased earthquake action for the isolated bridges depending on the soil condition and the natural period of the bridge, in addition to the philosophy of the Menshin design to achieve inertia force reduction primarily by means of enhancement of damping capability. This concept is further extended to limit the restoring force element as much as possible, and a high level of structural damping is introduced with the use of high capacity energy dissipation devices, in order to utilize effective reduction effects of seismic forces by isolation. This concept has been proposed as the Isolation Seismic Controlled Slide System (ICSS) (Matsuda et al., 2011). In this paper, the roles and contribution of the three devices in ICSS, namely the slide bearings, elastomeric bearings with energy dissipation capability, and seismic dampers, are investigated by means of dynamic response analysis using an example of 18-span continuous girder bridge application.

2. CONCEPT OF ICSS

Generally, the girder elongation and contraction due to temperature change, shrinkage, creep, etc. on long multi-span continuous girder bridge supported by seismic isolation bearings or elastomeric bearings induce statically indeterminate force acting on the substructures. As a result, it causes unfavorable effects on bearing displacements and post-yield response of the piers during an earthquake (Uno et al., 2010). On the other hand, the long multi-span continuous girder bridge with ICSS applications has a great advantage in diminishing the statically indeterminate force shown in Figure 2.1 with the use of an appropriate combination with isolation bearings, seismic dampers and sliding bearings (Matsuda et al., 2012). Utilizing this system, the following technical issues will be alleviated.

- 1) Since the statically indeterminate force due to elongation and contraction of the girder caused by temperature change etc. is significantly reduced, its harmful influence on the seismic performance of the bridge is mitigated.
- 2) Since the statically indeterminate force becomes negligible, need of adjustment of the bearing positions by post-slide method etc. during a construction can be eliminated.
- 3) The substructures supporting slide bearings can be slimmed down, and although the substructures supporting elastomeric bearings and seismic dampers become larger, the scale and cost of the substructure system can be reduced.
- 4) A high level of structural damping is achieved by means of the nonlinear energy dissipation mechanism of the devices.

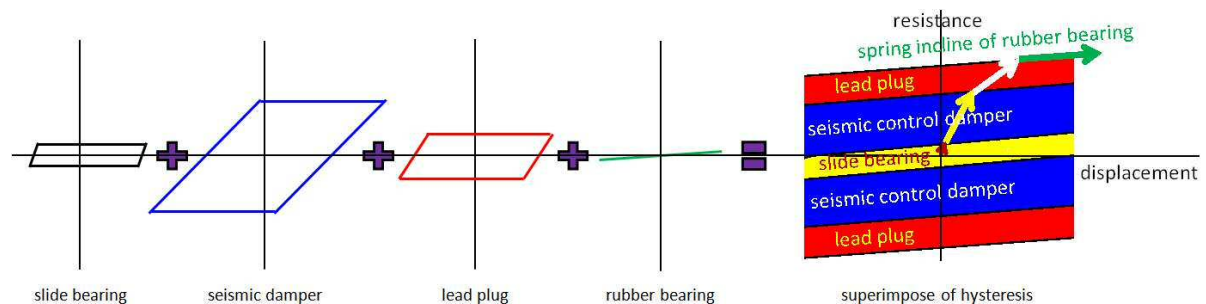


Figure 2.1 Example of application of each device in ICSS

3. RESPONSE MODIFICATION DEVICES ON ICSS

The characteristics of each device used for bearing can be described as follows.

1) Isolation Bearings

The lead elastomeric bearing (LRB) is applied as the elastomeric bearing with energy dissipation capability. The LRB consists of a natural laminated rubber and lead plugs. The elastomeric bearing is a nearly elastic element without energy absorption capability while the lead plugs are regarded to have only energy absorption capability.

2) Seismic Dampers

The friction type hysteretic damper utilizing Bingham fluid is adopted as the seismic damper. The resistance force of the damper employed for the analysis is assumed to be proportional to 0.1th power of velocity.

3) Slide Bearing

The superstructure is isolated from the substructures by employing slide material with small friction coefficients. The friction coefficient of slide bearings assumed in this system ranges between 0.01-0.05 depending on the sliding velocity.

The inertia force resisted by each device can be divided as shown in Figure 3.1. The function of each device is activated in the order of slide bearings, seismic dampers, and lead plugs in accordance with the initial rigidity. After yielding of all these devices, the laminated rubber part generates resilient forces in addition to the almost constant resistance forces during the deformation.

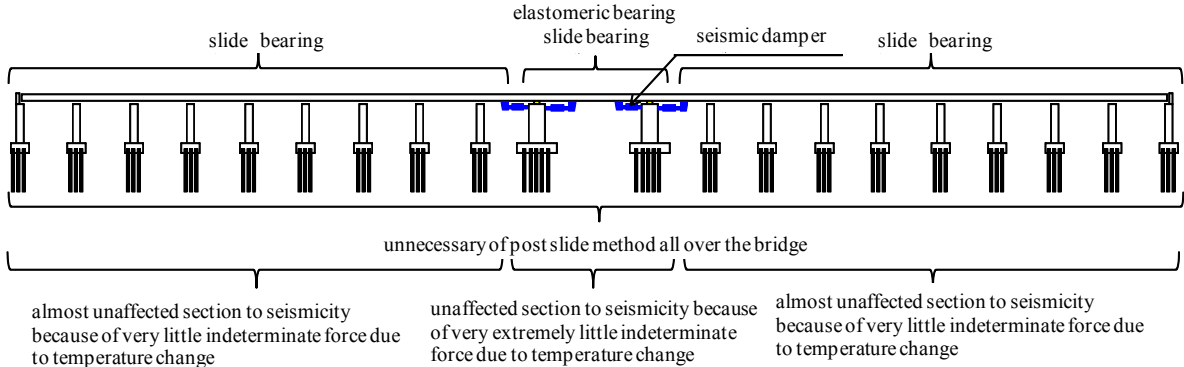


Figure 3.1 Superpose of the device history characteristic and concept of resistance on ICSS

4. BRIDGE AND CONDITIONS FOR RESEARCH

In order to evaluate the functions of the devices in ICSS, case study using a bridge model is carried out. The bridge employed for the case study is an 18-span continuous steel girder bridge shown in Figure 4.1 For the center spans between P8 and P11 that cross over the river, box girders are employed in view of a comparatively long span length of 135.5m. For the other spans, 2-steel plate girders are used.

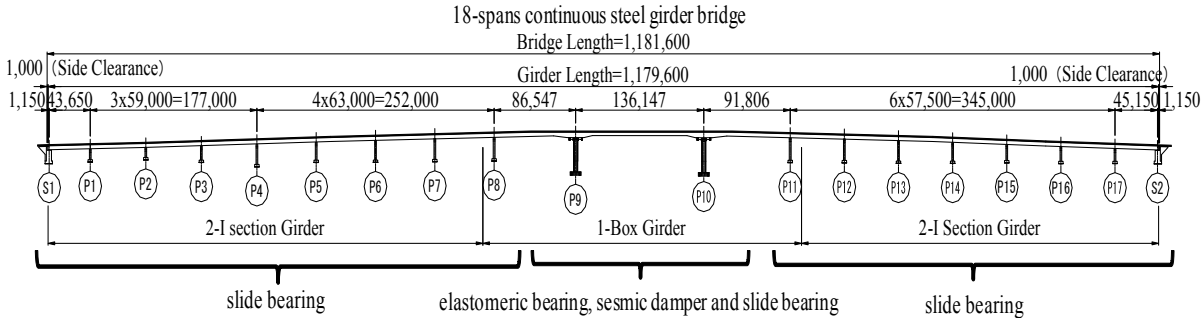


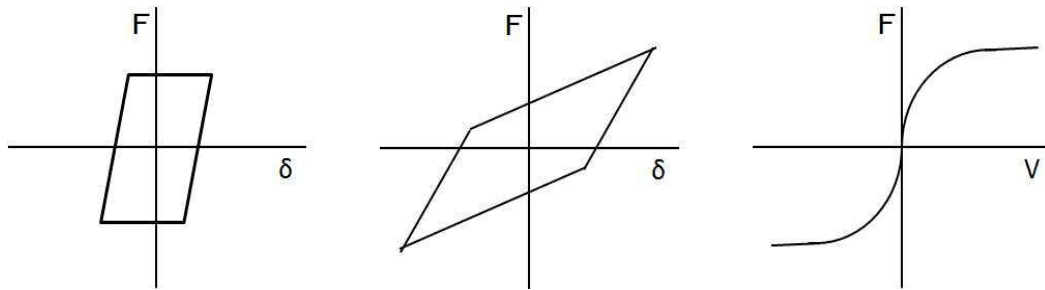
Figure 4.1 Bridge model

4.1. Arrangement of response modification devices

The layout of the devices is shown in Figure 4.1, and the transverse displacements at both girder ends are restrained on the abutments.

4.2. Response modification devices

The hysteretic behaviors of slide bearing, isolation bearing and seismic damper installed on P9 and P10 are shown in Figure 4.2 .



a) Slide bearing (b) elastomeric bearing (c) seismic damper

Figure 4.2 Restore characteristics of devices

Detail of each response modification device is described.

1) Elastmeric Bearing

The LRB of dimensions $1,600 \times 2,600$ mm, and total rubber thickness =325 mm (13-layers \times 25 mm) are assumed to be used

One unit is installed on P9 and P10, respectively.

The restoring force characteristics are modelled by a bilinear model with parameters at 250 % shear deformation.

2) Seismic Damper

The force of the seismic dampers is modelled by Eqn. (4.1). The distance between the end set pins is 3.85 m. These are installed in the orientation of 45 degrees from the local bridge axis.

$$F = C \cdot V^{0.1} \quad (4.1)$$

Where, F : Resistance Force (kN) (6000 kN at velocity 50 kine)

C : Reduction Coefficient ($\text{kN} \cdot \text{s}^{0.1} / \text{m}^{0.1}$)

V : Velocity (m/s)

3) Slide Bearing

The behavior of slide bearings is characterized by the friction coefficient of 0.05 with a elasto-perfectly plastic model of yield displacement of 2.5mm.

4.3. Restoring force characteristics of Piers

The layout of rebars in piers P9 and P10, to which the isolation bearings and seismic dampers are installed is shown in Figure 4.3. The $M-\phi$ model of the piers is shown in Figure 4.4 and the nonlinearity in each direction are considered independently without interaction. The Takeda type tri-linear model and SR foundation spring model on Type III ground are used in the analysis.

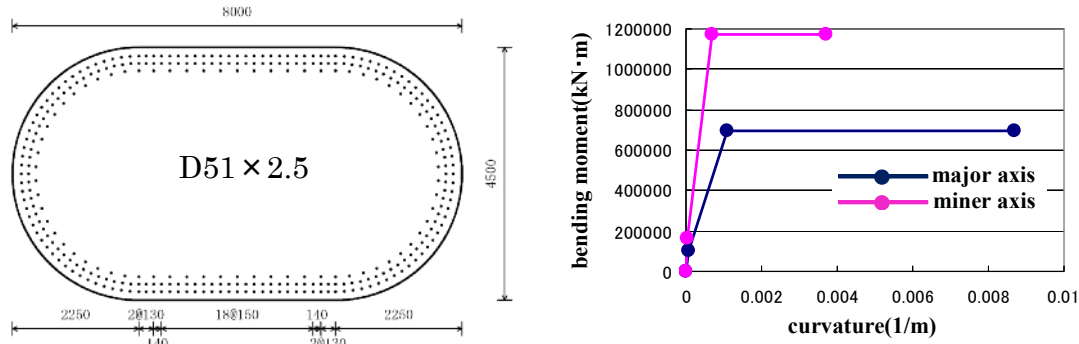


Figure 4.3 Arrangement of deformed steel bar in piers P9 and P10 **Figure 4.4** M- ϕ characteristics of pier

4.4. Seismic wave and input directions

The input seismic ground motion used in the analysis is the standard wave of Type II of Level 2 Earthquake Ground Motion of the III kind foundation (referred to as II-III-1) specified in Japan Specifications for Highway Bridges (Japan Road Association, 2002). Although the actual seismic ground motion is supposed to be three-dimensional (Igarashi et al., 2012), a uni-directional input is assumed in accordance with the dynamic analysis method designated in Japan Specifications for Highway Bridges in this paper. The dynamic analysis is conducted for the cases of four directions of input ground motion, with incident angles equally spaced at 45 degrees measured from the line connections the two abutments A1 and A2. These directions are selected in consideration of the curved alignment of the girder, installation of the seismic damper in an oblique direction, and significantly large displacements of the superstructure.

4.5. Eigen value analysis and Rayleigh damping constants

Only the elastomeric bearings are taken into consideration in the evaluation of the damping characteristic using Rayleigh damping. The equivalent damping ratios of the superstructure, the pier, the isolation bearing and the foundation are 2%, 2%, 10% and 5%, respectively. The fundamental natural period of the system in the longitudinal, transverse and vertical directions are 5.3 sec, 16.3 sec and 1.6 sec, respectively. Rayleigh damping constants are $\alpha = 0.016667$ and $\beta = 0.00654$ determined by the 1st and 38th modes. The dynamic response of the model is analysed by means of the nonlinear step-by-step time history response analysis using the Newmark- β method ($\beta = 1/4$) with the step interval of $\Delta t = 0.001$ sec, accounting for finite deformation.

5. FUNDAMENTAL RESPONSES OF DEVICES

5.1. Time history response displacement

The displacement time histories in the longitudinal and transverse directions at the center of the superstructure on the top of pier P9 are shown in Figure 5.1 and Figure 5.2, respectively.

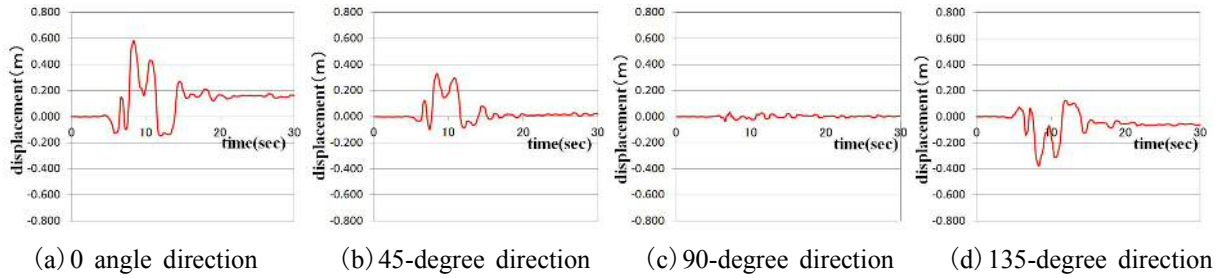


Figure 5.1 Response displacement time history (P9, longitudinal component)

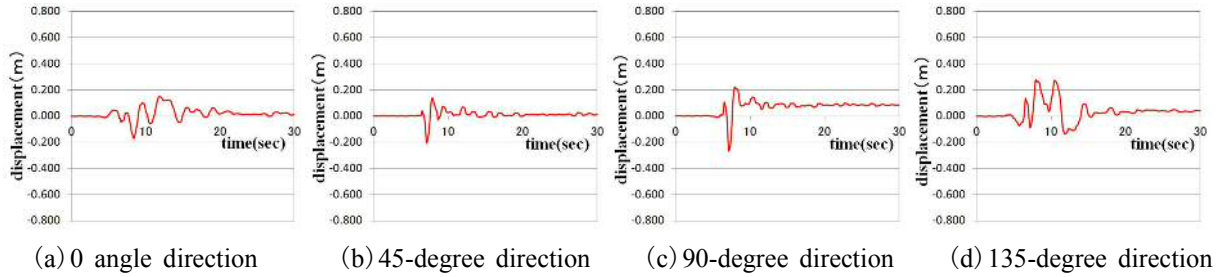


Figure 5.2 Response displacement time history (P9, transverse component)

5.2. Resistance force Time history

The resistance force time histories of the response modification devices at pier P9 during the time segment 0-30 sec are shown in Figures 5.3 and 5.4. The absolute values of each component are plotted in the figure. It is anticipated that the devices resist in sequence as shown in Figure 5.5. On the other hand, the time history of the resistance force shown in Figure 5.6 indicates that the resistance force of the laminated rubber part gradually increase after the lead plugs reach to the yield load. Resistance force of the seismic dampers keep changing until the maximum displacement, and especially a rapid drop of the damper force can be seen just before the maximum displacement. This can be explained by the velocity dependence of the seismic damper force. It is well indicated by velocity response which is also plotted in Figure 5.6.

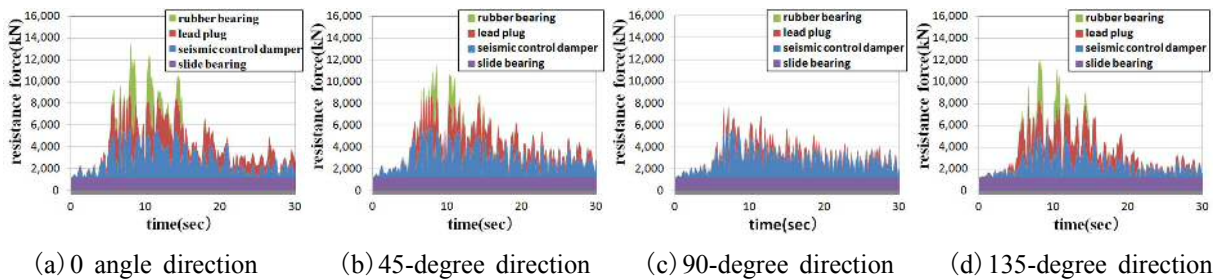


Figure 5.3 Time history of resistance forces during 0-30 sec on each device (P9, longitudinal component)

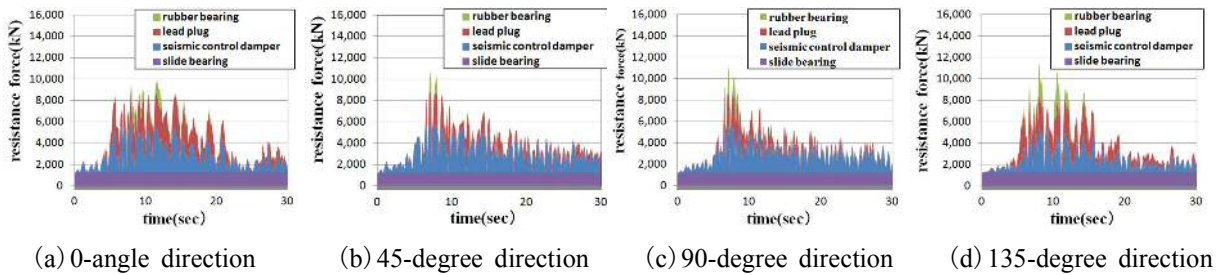


Figure 5.4 Time history of resistance forces during 0-30 sec for each device (P9, transverse component)

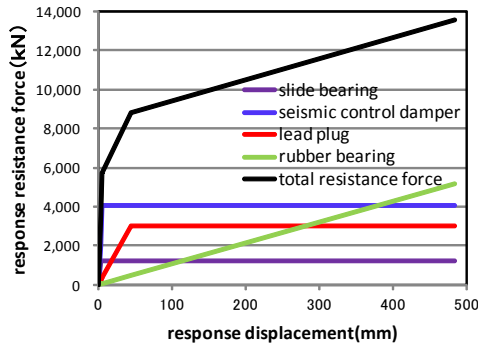


Figure 5.5 Relationship between resisting force and maximum resistance (P9)

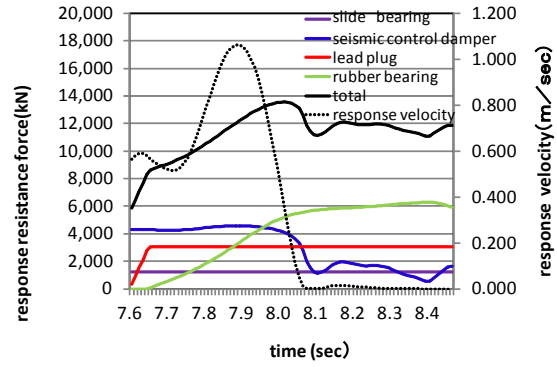
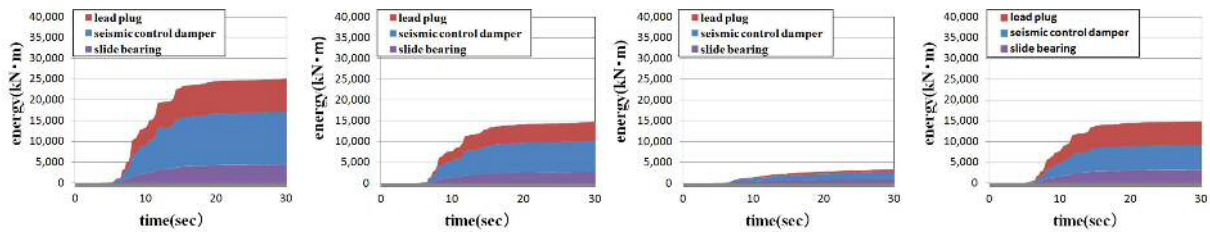


Figure 5.6 Close-up of time history of resistance force (P9)

6. DISCUSSION ON SYSTEM RESPONSE

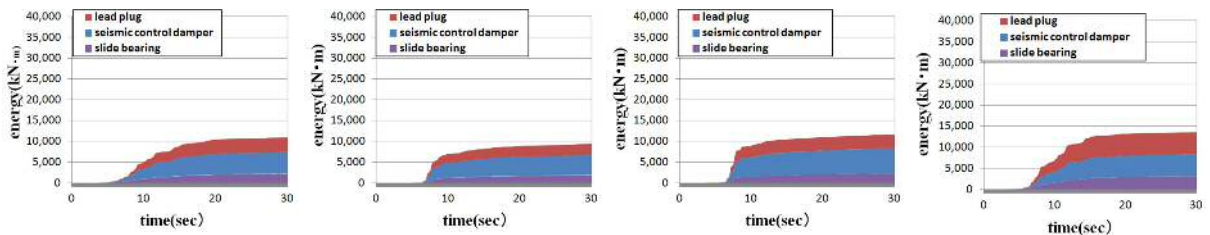
6.1. Cumulative energy absorption

The energy absorbed by each device at pier P9 during 0-30 sec is shown in Figures 6.1, 6.2, and 6.3. The energy absorbed by seismic dampers is the largest among the three devices. The amount of the absorbed energy is almost unaffected by the input direction.



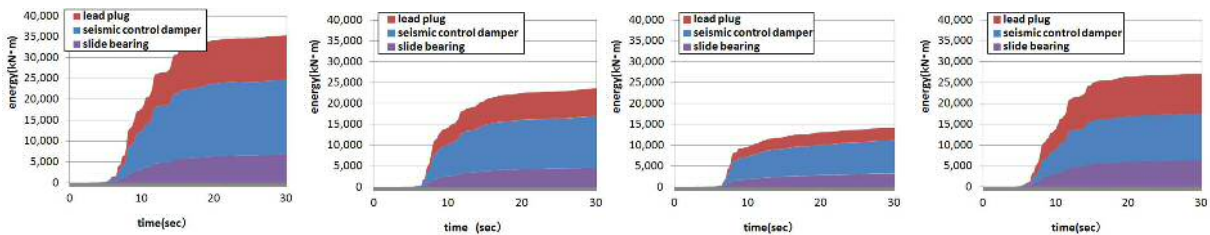
(a) 0 angle direction (b) 45-degree direction (c) 90-degree direction (d) 135-degree direction

Figure 6.1 Absorbed energy by each device (P9, longitudinal component)



(a) 0 angle direction (b) 45-degree direction (c) 90-degree direction (d) 135-degree direction

Figure 6.2 Absorbed energy by each device (P9, transverse component)



(a) 0 angle direction (b) 45-degree direction (c) 90-degree direction (d) 135-degree direction

Figure 6.3 Total absorbed energy by each device (P9)

6.2. Input direction and maximum resistance forces

Comparison of the maximum resistance forces for different input directions are shown in Figure 6.4. Noticeable difference among the cases can be seen in the contribution of the devices, in particular the maximum response resistance forces of elastomeric bearing show significant variation. In contrast to the other devices that tend to generate constant forces after yielding, the laminated rubber part of the elastomeric bearing induces restoring force proportional to the displacement.

6.3. Equivalent damping ratios

The hysteresis loops of the devices with the calculated maximum response amplitudes to evaluate are used the equivalent damping ratios based on the Eqn. (6.2) defined in Japan Specifications for Highway Bridges. The plots of ΔW , $2\pi W$ and equivalent damping ratios are shown in Figure 6.5 and Figure 6.6, respectively. This figure shows that small values of the equivalent damping ratios are obtained for greater displacement response cases, and energy dissipation due to friction-type hysteresis becomes dominant in the cases which the displacement of the rubber is small, resulting in the equivalent damping ratios close to 0.6, the characteristic value of pure friction case.

$$h_B = \frac{\Delta W}{2\pi W} \quad (6.2)$$

Where, h_B : equivalent damping ratio

W : elastic strain energy at the maximum displacement

ΔW : absorbed energy per cycle

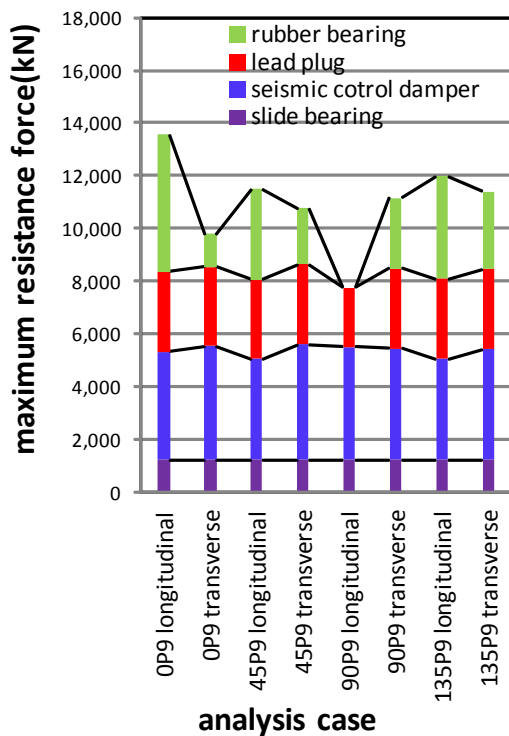


Figure 6.4 Maximum resistance forces

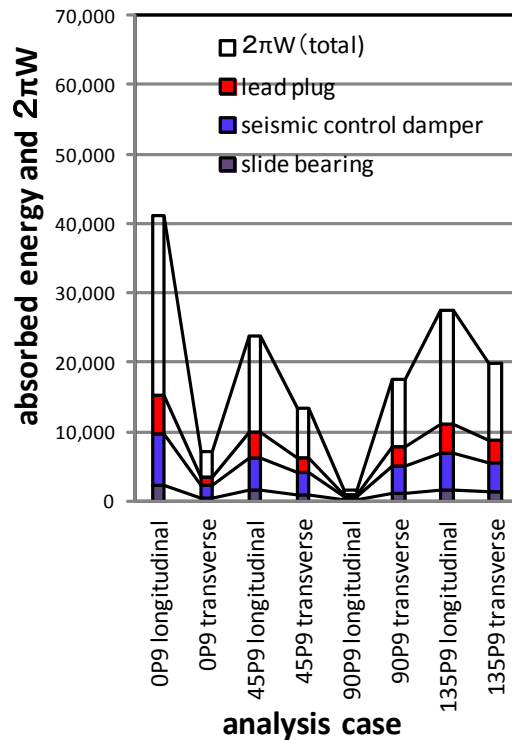


Figure 6.5 Absorbed energy

6.4. Inertia force reduction effect of the energy dissipation

As the effects of the inertia force reduction by the response modification devices represented by equivalent damping ratios are shown in Figure 6.7. In the evaluation, the acceleration reduction factors according to damping ratio given by the Eqn. (6.3) used in Japan Specifications for Highway Bridges are adopted as a rough estimate of general trends. The acceleration reduction factor due to the damping ratios of each device is considerably smaller than unity and the reduction factor for the entire system is as low as 0.6, showing sufficient reduction performance.

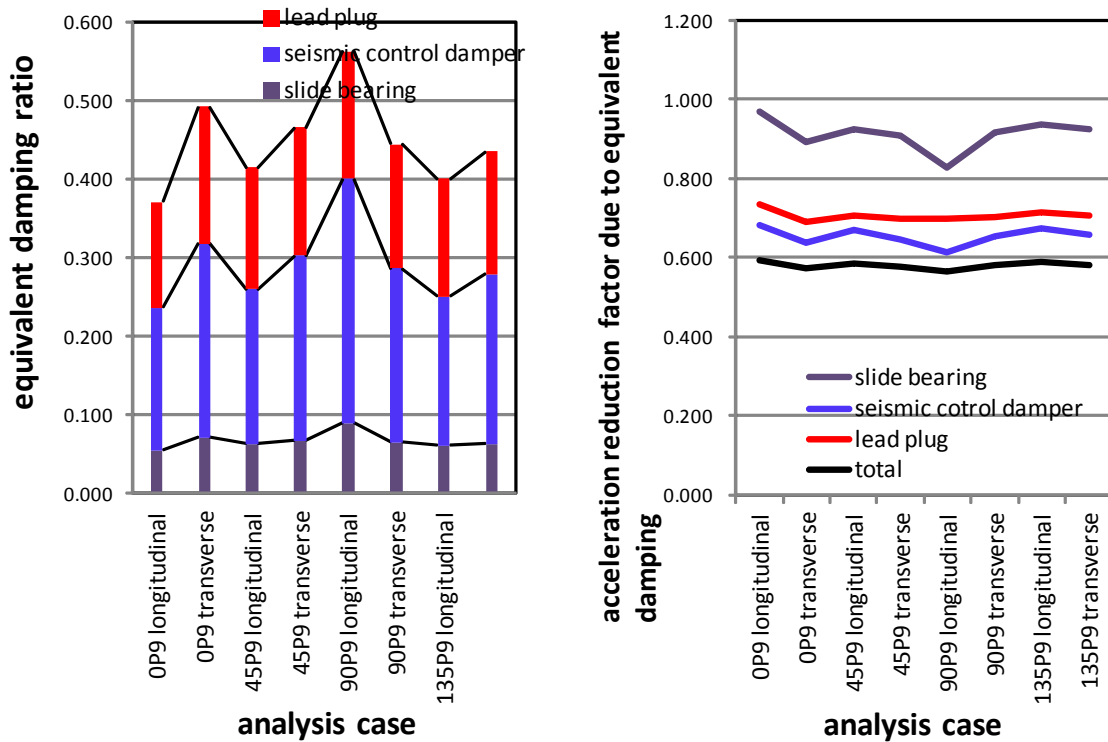


Figure 6.6 Equivalent damping ratio Figure 6.7 Evaluation of spectral acceleration reduction factor

$$C_d = \frac{1.5}{40h + 1} + 0.5 \quad (6.3)$$

Which, C_d : Spectral acceleration reduction factor due to damping ratio
 h : Equivalent damping ratio

7. CONCLUSION

The findings on the response of ICSS described in this paper can be summarized as follows.

- 1) The slide bearings, seismic dampers and lead plugs are effective in generating the resisting force even with a small displacement. The elastomeric bearing resists to the inertia forces exceeding the forces due to the other devices.
- 2) The absorbed energy greater by slide bearings, seismic dampers and lead plugs is significant. In this case study, 30 % or greater equivalent damping ratios are obtained in all cases. As a result, it is estimated that inertial forces of the superstructure are reduced by the factor of 0.6.
- 3) Although the resistance forces of the seismic dampers decrease rapidly when the resistance force of the bearings approaches to the maximum, the change of total resistance force of the bearings is

small. This can be explained by the velocity dependence the resistance force of the seismic damper.

Since the seismic dampers are expected to generate a high level of resistance force in ICSS, significant effective damping performance is shown to be obtained and contributes to the enhancement of the seismic performance of the bridge. Research on the optimized parameters of each response modification device so that the required performance of the bridge can be effectively satisfied is the subject of further study on ICSS.

REFERENCES

- Japan Road Association. (2002). Specifications for Highway Bridges. Seismic Design (in Japanese).
- Uno, H. Mazda, T. Miyamoto, H. Yunoki, K. Chou, S. Shinoda, R. (2010). Seismic behavior of bridges due to girder elongation and shrinkage caused by temperature changes. *Proceedings of 5th World Conference on Structural Control and Monitoring*. No.149. 1-12.
- Matsuda, T. Ugai, K. Wada, Y. Uno, H. and Matsuda, H.(2011). Concept and fundamental characteristics of ICSS adapted for super long continuous curved bridge. *Proceedings of 14th Symposium on Ductility Design Method for Bridges*.199-206.
- Matsuda, T. Igarashi, A. Ueda, Y. Miyazaki, S. and Matsuda, H.(2012). A study on functions of response modification devices of bridge adapted for ICSS. *Journal of JSCE*. Ser. A1. (to appear).
- Ouchi, H. Ueda, T. Wada, Y. Igarashi, A. Matsuda, T. Sakate, M. Uno, H. and Matsuda, H. (2012). ICSS (1) Concept and fundamental characteristics of seismic response. *Proceedings of 15th World Conference on Earthquake Engineering*.
- Sakate, M. Igarashi, A. Ouchi, H. Ueda, T. wada, T. Matsuda, T. Uno, H. and Matsuda, H. (2012). ICSS (3) Seismic response to bidirectional input ground motions. *Proceedings of 15th World Conference on Earthquake Engineering*.
- Tsushima, D. Igarashi, A. Ouchi, H. Ueda, T. wada, Y. Matsuda, T. (2012). ICSS (4) A design applied for super long multi-span bridge. *Proceedings of 15th World Conference on Earthquake Engineering*.
- Igarashi, A. Inoue, K. Furukawa, A. Uno, H. and Matsuda, H. (2012). Synthesis of bidirectional seismic ground motion by standard and complementary waves for seismic design of bridges. *Proceedings of 15th World Conference on Earthquake Engineering*.